J Solid State Electrochem (2010) 14:1255–1260
DOI 10.1007/s10008-009-0928-9

ORIGINAL PAPER

Electrochemical behavior of aluminum alloy AA2024 in aqueous solutions in the presence of caffeine

Rondon Sabino · Denise Schermann Azambuja · Reinaldo Simões Gonçalves

Received: 8 July 2009 / Revised: 18 August 2009 / Accepted: 24 August 2009 / Published online: 19 September 2009
© Springer-Verlag 2009

Abstract The influence of the presence of caffeine (CFN) on the electrochemical behavior of aluminum alloy AA2024 in aqueous solutions was studied. The interaction between the metal surface and the organic compound is potential dependent as well as time dependent. The anodic currents, responsible for the metal dissolution, decreases in the presence of caffeine even adding chloride anion as contaminant. The EIS data obtained at the open-circuit potential clearly demonstrated that the adsorption of CFN on the surface of the AA 2024 electrode is favored allowing the film defects to be repaired. The protective action of CFN is considerably improved on increasing the adsorption time due to a sealing process which enhances the film stability.

Keywords Aluminum alloy · Electrochemical techniques · Adsorption · Caffeine

Introduction

Aluminum alloys are important materials used in many industrial applications. The aluminum alloy AA 2024 is extensively used due to its excellent weight-to-strength ratio [1]. However, the composition of this alloy makes it very prone to corrosion processes. The intermetallic particles cover about 3% of the geometric surface area of the alloy [1], Al_2CuMg being the predominant type, followed by Al_6 (Cu, Fe, Mn). Thus, the corrosion starts in the zone of intermetallic particles. The salts of rare earth elements, such as cerium and lanthanum, have been found to provide an effective corrosion inhibition for the aluminum alloys [2].

Organic compounds are recognized as effective inhibitors of the corrosion of many metals and alloys. The efficiency of an organic compound as a corrosion inhibitor is closely associated with the chemical adsorption [3–7]. Most of these organic compounds contain nitrogen, sulfur, oxygen, and multiple bonds in the molecules which are adsorbed on the metal surface or act in chelating reactions between the metal surface and the organic compound [8, 9]. It has been reported that a mixture of benzotriazole and 8-hydroxyquinoleine has a synergistic effect on AA 2024 corrosion inhibition, acting on both the cathodic and anodic reaction [10]. Many studies have been conducted to examine some naturally occurring substances in order to find environmentally safe substances which can act as corrosion inhibitors for different metals in a variety of environments [8, 11–16].

Our laboratory has previously investigated the interaction of caffeine (CFN) with copper in aqueous medium. The efficiency of caffeine was experimentally confirmed [17]. This paper reports electrochemical evidence of the ability of caffeine (see Fig. 1 for structural formula) to inhibit the corrosion of AA 2024 in aqueous sodium sulfate solutions. The interaction between the organic compound and the metal surface was characterized by means of cyclic voltammetry and electrochemical impedance spectroscopy (EIS).

R. Sabino · D. S. Azambuja · R. S. Gonçalves (✉)
Universidade Federal do Rio Grande do Sul,
Av. Bento Gonçalves, 9500, Caixa Postal 15049,
CEP 91501-970 Porto Alegre, RS, Brazil
e-mail: reinaldo@iq.ufrgs.br

Fig. 1 Caffeine (1,3,7 trimethylxanthine)

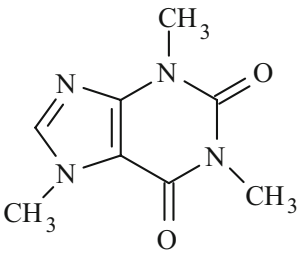

Experimental

Materials

Working electrodes for cyclic voltammetry and electrochemical impedance spectroscopy were cut, in a rectangular shape (2.5 cm×1.0 cm×0.1 cm), from a commercial aluminum alloy AA 2024 sheet. This alloy is characterized by an aluminum matrix with a chemical composition (wt.%) of 3.8–4.9 Cu, 1.2–1.8 Mg, 0.3–0.9 Mn, 0.5 Fe, and 0.5 Si. The working electrodes were polished with 1200 emery paper, rinsed with deionized water and degreased with p.a. grade acetone:chloroform (1:1) mixture obtained from Nuclear, prior to each experiment. The caffeine was supplied by Acrós Organics (98.5% pure). All solutions were prepared using deionized water. The electrical conductivity of aqueous solutions was increased by addition of 0.10 mol L^{-1} sodium sulfate (Merck), as the supporting electrolyte. Some tests were conducted in the presence of diluted sodium chloride (ECIBRA) in order to increase the aggressivity of the medium. All experiments were performed at room temperature (25 °C) with aerated aqueous solutions.

Apparatus

The electrochemical set-up consisted of an Autolab potentiostat; model PGSTAT30, coupled to a personal computer. A glass three-electrode electrochemical cell was used. A platinum wire was employed as the auxiliary electrode and an Ag/AgCl was used as the reference electrode.

Results and discussion

Cyclic voltammetry

Electrochemical behavior of aluminum alloy

In order to gain an understanding of the electrochemical profile of the aluminum alloy 2024 these experiments were important to characterize the reduction and oxidation processes occurring on the metal surface. Figure 2 shows the cyclic voltammograms of the alloy in 0.10 mol L^{-1} sodium sulfate recorded at 0.10 Vs^{-1} after keeping the electrode polarized for two different time periods (adsorption time, t^{ads}=0 s and 30 s) at the initial potential. All experiments with cyclic voltammetry were carried out using these values for sweep rate and t^{ads}, under static conditions. The potential range used was previously determined as that which gave the best adsorption of the organic compound on the electrode surface.

As observed in Fig. 2 during the anodic potential sweep, positive current densities associated with aluminum oxide formation were observed. These currents refer to the charge transfer process associated with the oxidation reaction of the metal (see Eq. 1). The onset of this process occurs at E=−0.36 V (Ag/AgCl) for $t^{ads} = 0$s and $E = -0.50$V (Ag/AgCl) for $t^{ads} = 30$s. These values refer to the point at which the current value is zero and were determined directly from the voltammograms. The influence of the adsorption time may be explained considering the presence of different adsorbed species on the metal surface mainly after maintaining the electrode polarized for 30 s at the initial potential. It is likely that during this time adsorbed hydrogen is accumulated on the metal surface. Following the potential sweep in the positive direction an anodic current peak was observed at $E^{peak} = 0.11\text{V(Ag/AgCl)}$ for $t^{ads} = 0$ s and $E^{peak} = 0.13\text{V(Ag/AgCl)}$ for $t^{ads} = 30$s. At these potential values the most probable anodic reaction involves the charge transfer associated with the oxidation of the metal:

$$4Al + 6H_2O + 3O_2 \rightarrow 4Al(OH)_3 \quad (1)$$

The mechanism of oxide layer growth involves the presence of the solvent on the electrode surface similarly to that previously proposed for iron oxidation in aqueous

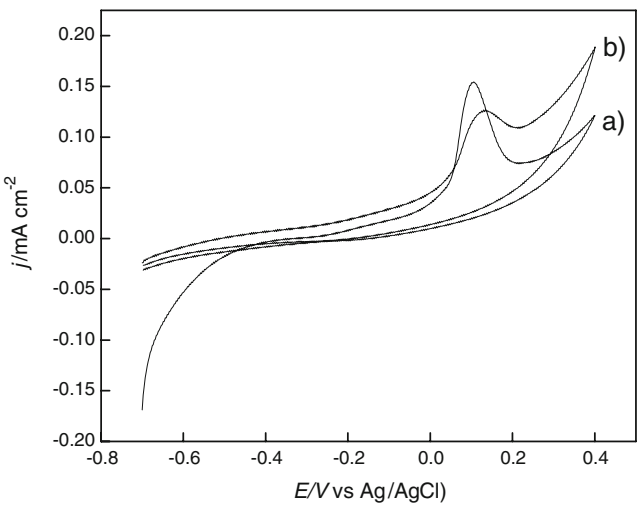

Fig. 2 Cyclic voltammograms of the aluminum alloy AA 2024 recorded at 0.10 Vs^{-1}, in aqueous 0.10 mol L^{-1} Na_2SO_4, after (*a*) t^{ads}= 0 s and (*b*) t^{ads}=30 s

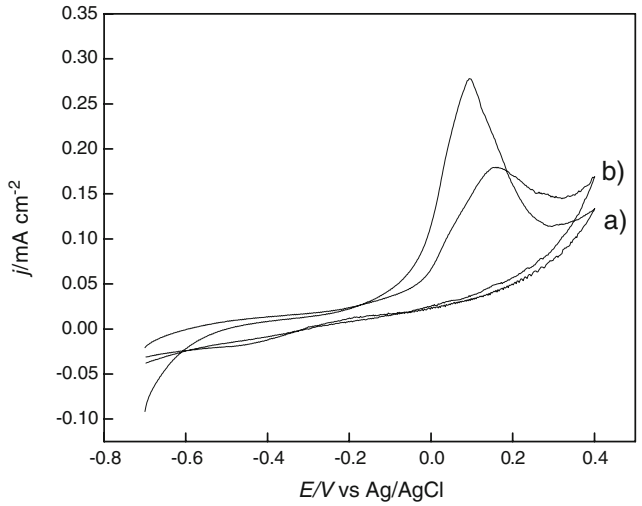

Fig. 3 Cyclic voltammograms of the aluminum alloy AA 2024 recorded at 0.10 Vs^{-1}, in aqueous 0.10 mol L^{-1} Na_2SO_4 containing 100 ppm of chloride, after (*a*) t^{ads}=0 s and (*b*) t^{ads}=30 s

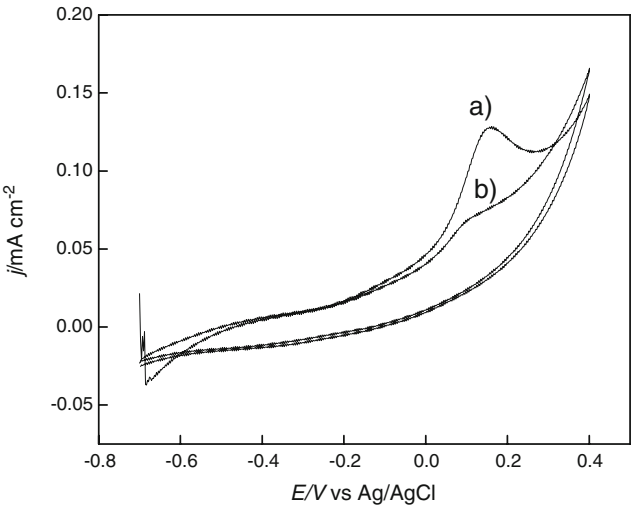

Fig. 5 Cyclic voltammograms of aluminum alloy AA 2024 recorded at 0.10 Vs^{-1}, in the presence of 10 mmol L^{-1}caffeine: (*a*) t^{ads}=0 s; (*b*) t^{ads}=30 s

medium [6]. Comparing the two voltammograms the peak anodic current values were lower after 30 s at the initial potential. This may be due to a blocking effect of the adsorbed hydrogen. This species could be formed on the surface since the electrode is being polarized cathodically. The water adsorption involved in the aluminum hydroxide formation (Eq. 1) decreases proportionally. However, at more positive potential the anodic current values increase, as seen by comparing both curves. This effect probably means that the oxide layer is being dissolved as aluminum salt.

During the negative potential sweep, cathodic currents associated with reduction processes were observed starting at −0.20 V (Ag/AgCl) for both adsorption times. However, it is visible that the voltammogram profiles suggest an irreversible process in this potential range.

Some experiments were repeated with the addition of chloride (100 ppm) as shown in Fig. 3.

As observed from the voltammograms the anodic current values at the peak potential are almost twice the values observed on the voltammograms in the absence of chloride (Fig. 2) for both adsorption time periods. These findings are

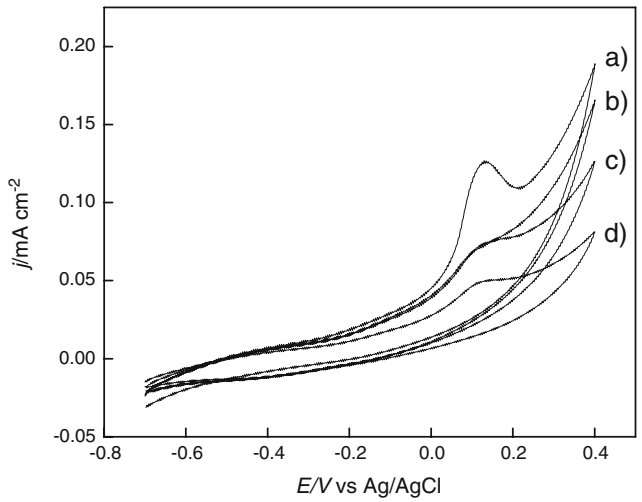

Fig. 4 Cyclic voltammograms of the aluminum alloy AA 2024 recorded at 0.10 Vs^{-1}, in aqueous 0.10 mol L^{-1} Na_2SO_4: (*a*) in the absence of caffeine, and in the presence of caffeine at concentrations of (*b*) 10 mmol L^{-1}, (*c*) 15 mmol L^{-1}, and (*d*) 20 mmol L^{-1} after maintaining the initial potential for 30 s

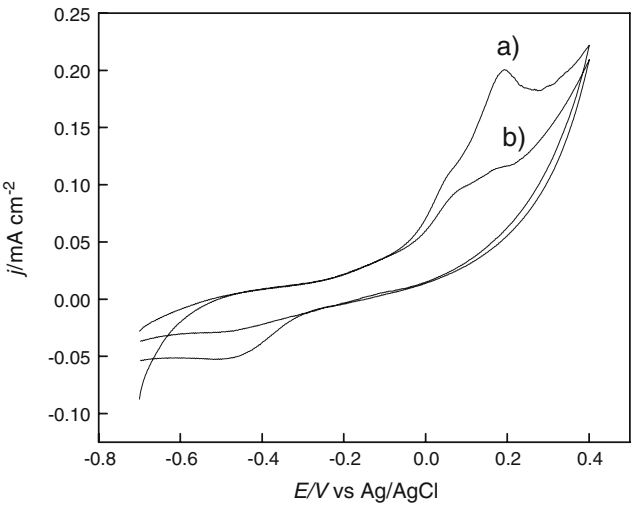

Fig. 6 Cyclic voltammograms of aluminum alloy recorded at 0.10 Vs^{-1}, in the presence of 100 ppm of chloride and 10 mmol L^{-1} caffeine: (*a*) t^{ads}=0 s; (*b*) t^{ads}=30 s

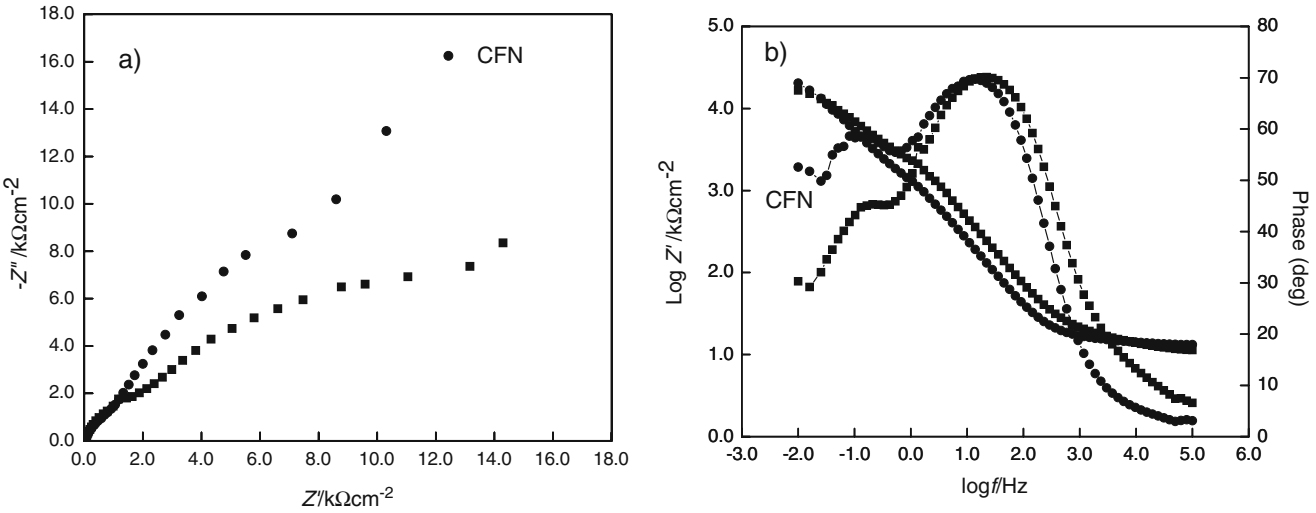

Fig. 7 The Nyquist (**a**) and Bode (**b**) diagrams of aluminum alloy at OCP, in aqueous solution containing 0.10 mol L^{-1} of Na_2SO_4 in the absence and in the presence of 10 mmol L^{-1} of caffeine

in agreement with the literature, which report [18] that when the AA2024 alloy was polarized in sulfate solutions the intermetallic particles were homogeneously dissolved, and when chloride ions were added, pits were formed preferentially on these particles, due to a synergetic effect of SO_4^{2-} and Cl^- ions toward copper. Buccheit et al. [19] proposed that a selective dissolution of copper- and magnesium-rich particles led to the formation of a highly porous copper-rich layer at the surface of the alloy.

Effect of the presence of caffeine

The first step for this effect was to find the best conditions for the interaction between the organic compound and the electrode surface. The strategy was first determining the potential program in order to get the highest inhibitory effect. The dependence of the interaction between the corrosion inhibitor and the metal surface on the initial potential has been described previously [3]. The best condition was observed when the electrode was polarized at −0.70 V (Ag/AgCl).

The effect of the presence of caffeine at different concentrations on the electrochemical behavior of the aluminum alloy in this medium and under these conditions is shown in Fig. 4.

The presence of caffeine decreases considerably the anodic processes associated with the electrooxidation of the aluminum alloy, mainly after maintaining the electrode at the initial potential for 30 s. The interaction between the organic compound and the electrode surface should affect the corrosion potential value, shifting to more positive (negative) values. However, this effect was not remarkable.

The anodic current values at the corrosion peak (E= 0.10 V) decreases almost proportionally to the caffeine concentration. This same effect was observed even at more positive potential (E=0.40 V). Assuming that the current at this potential is associated with the oxide layer dissolution it is clear that the presence of caffeine decreases these current values and almost proportionally regarding to the caffeine concentration. This may corroborate that less oxide layer is being formed in the presence of the organic compound.

In order to evaluate the effect of the time where the electrode potential is kept constant during the adsorption processes of caffeine on the aluminum alloy, some experiments were performed. The effect of (t^{ads}) on the anodic current values in the presence of caffeine is unequivocally explained by comparing the voltammograms shown in Fig. 5.

The presence of 10 mmol L^{-1} of caffeine decreases the anodic current values; however, this effect was more pronounced after keeping the electrode potential for 30 s at −0.70 V (Ag/AgCl). This should mean that the electrode surface is being recovered by the organic compound trough out a slow adsorption process.

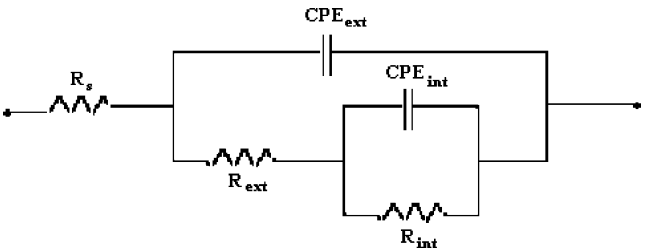

Fig. 8 Equivalent circuit used to fit the EIS data for aluminum alloy given in Fig. 7

Table 1 Simulated values used in the equivalent circuit given in Fig. 7

C^{CFN}/mM	$R_{.}^{elect}$/Ωcm^2	$R_{.}^{ext}$/kΩcm^2	CPE^{ext}/μFcm^{-2}	n	R^{int}/kΩ cm^2	CPE^{int}/μF cm^{-2}	n
Blank	12.7	6.32	7.38	0.79	12.37	298	0.49
10	13.9	4.81	19.8	0.81	27.05	135	0.66

The same experiment was repeated in the presence of small amount of chloride ion as is showed in Fig. 6.

The same comments should be applied here. The interaction between the electrode surface and the organic compound is time dependent even in the presence of chloride. This conclusion is visible by comparing the current density values recorded at the anodic potential peak. However, a new electroreduction process around −0.50 V (Ag/AgCl) was observed in the presence of chloride during the cathodic potential sweep. In order to explain this peak it is plausible to infer that the only species that may be involved in this process is the caffeine molecule. The presence of chloride may induce an electronic delocalization in such a way to compel the caffeine molecule to adsorb on the electrode surface differently as compared with the adsorption way in absence of the ion. As consequence, a charge transfer processes should occur towards the unsaturated bonds.

Electrochemical impedance spectroscopy results

Effect of the presence of caffeine

EIS spectra of the alloy were recorded at the open-circuit potential (OCP) after 30 min immersion in aqueous 0.10 mol L^{-1} Na_2SO_4 with and without the addition of 10 mmol L^{-1} CFN (t^{ads}=60 s). The Nyquist diagrams (Fig. 7a) show two deformed capacitive loops, the first one at higher frequencies related to an inner thin barrier-type layer and the second one in the low frequency range related to a thicker outer porous layer. From the Bode plots (Fig. 7b) in the absence of CFN, a maximum phase angle close to −45° is detected at the low frequency range. This is characteristic of a diffusion-controlled process within the external oxide layer [20, 21]. On the other hand, in CFN-containing solutions, the maximum phase angle increases up to −60°, indicating that the contribution of diffusion to the overall process decreases.

The interpretation of the EIS plots of Fig. 7 was performed by numerical simulation, using an equivalent circuit (EC) composed by two time constants (Fig. 8). This EC was based on a two-layer model consisting of a barrier inner layer and a porous outer layer, as described elsewhere [22, 23].

In this EC (Fig. 8), R^s corresponds to the electrolyte resistance, the CPE is a constant phase element which replaces the capacitance of the external and internal layer, and R^{ext} and R^{int} are the respective resistance values for these layers.

The simulated data are given in Table 1. The CPE impedance is generally related to surface reactivity, surface roughness, electrode porosity, and to diffusion process. This

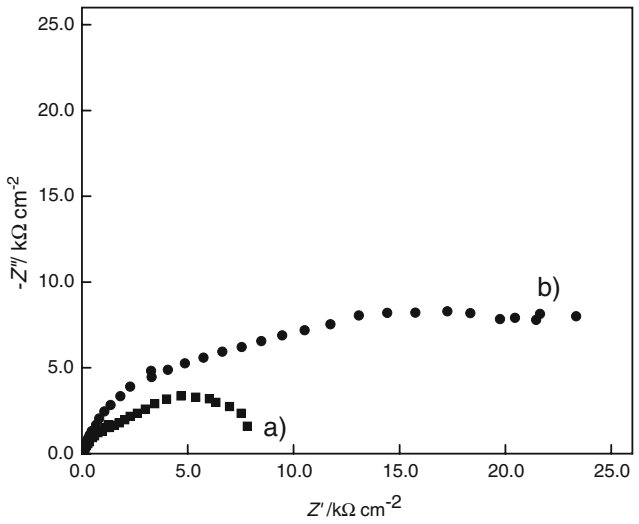

Fig. 9 Nyquist diagrams of aluminum alloy at *OCP* in aqueous solution of 0.10 mol L^{-1} Na_2SO_4 in the presence of 20 mmol L^{-1} of caffeine: (*a*) after t^{ads}=0 s and (*b*) t^{ads}=60 s of adsorption time

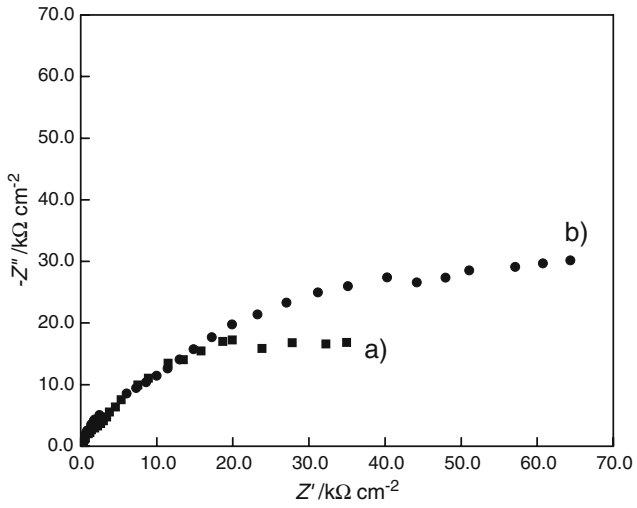

Fig. 10 Nyquist diagrams of aluminum alloy at OCP in aqueous 0.10 mol L^{-1} Na_2SO_4 solution with 100 ppm of NaCl: (*a*) in the absence and (*b*) in the presence of 20 mmol L^{-1} caffeine after 60 s of adsorption time

is given by $Z^{CPE}=[Q(j\omega)^n]^{-1}$ [24] where CPE represents an ideal capacitor for $n=1$, a resistor for $n=0$, and diffusion processes for $n=0.5$. As can be seen in the presence of 10 mM CFN the resistance of the outer layer increases from 12.4 to 27.1 kΩ cm^2 and the corresponding value for the CPE decreases from 293 to 135 μF cm^{-2}. Thus, in the presence of CFN the diffusion contribution to the overall process decreases due to the adsorption of this compound at the regions of the film with defects, producing a more protective film.

Effect of adsorption time

The effect of the CFN adsorption time on the electrochemical behavior of AA 2024 was evaluated. The procedure used was to adsorbed the CFN on the electrode surface for $t^{ads}=0$ s and 60 s at the adsorption potential, followed by immersion in the electrolyte for 60 min. This time interval was assumed to be sufficient for the growth of a significant amount of oxide layer on the surface. Figure 9 depicts the Nyquist diagrams obtained with a CFN concentration of 20 mM. The EIS data are in agreement with the voltammetric results previously given (see Fig. 5).

Using the same EC given in Fig. 8, it can be concluded, from the simulated parameters, that on increasing the adsorption time to 60 s the resistance of both layers increases, R^{int} from 3.8 to 15.5 kΩ cm^2 and R^{ext} from 4.9 to 11.7 kΩ cm^2, in the presence of CFN, followed by a decrease in the capacitances. This trend can be attributed to CFN adsorption at the regions with defects and/or in the pores of the passive film leading to a more protective layer.

Effect of the presence of chloride

The effect of CFN addition was evaluated in the chloride-containing solution using the procedure described above. Figure 10 shows the EIS spectra of AA 2024 in aqueous 0.10 mol L^{-1} Na_2SO_4 solution with 100 ppm of NaCl after 60 min of immersion ($t^{ads}=0$ s) in absence and, comparatively, in the presence of 20 mmol L^{-1} of CFN.

Both diagrams show depressed capacitive loops; however, with CFN addition the overall impedance is increased. The value of the resistive component of the impedance measured at a sufficiently low fixed frequency can be employed to evaluate the corrosion resistance. Considering that in this study the lowest frequency employed was 10 mHz, the resistance measured at this point was used to evaluate qualitatively the corrosion behavior. A comparison of the R^{10mHz} values for the alloy AA 2024 in the electrolyte without and with CFN shows that in the presence of the inhibitor this value increased almost twofold from 34.9 to 64.3 kΩ cm^2. This finding can be attributed to the incorporation of CFN in the damaged areas of the passive layer enhancing the corrosion resistance of the alloy.

Conclusions

This paper reports electrochemical evidence of the ability of caffeine to inhibit the corrosion of AA 2024 in aqueous sodium sulfate solutions. The presence of caffeine decreases considerably the anodic processes associated with the electrooxidation of the aluminum alloy, mainly after maintaining the electrode at the initial potential for 30 s. This effect was observed even in the presence of chloride anion as contaminant.

The inhibiting action of CFN results in a significant increase of the impedance modulus in the whole frequency domain. The EIS data obtained at the open-circuit potential clearly demonstrated that the adsorption of CFN on the surface of the AA 2024 electrode is favored allowing the film defects to be repaired. The protective action of CFN is considerably improved on increasing the adsorption time due to a sealing process which enhances the film stability.

References

1. Zandi RZ, Langroud AE, Rahimi A (2005) Prog Org Coat 53:286–291
2. Yasaku KA, Zheludkevich ML, Lamaka SV, Ferreira MGS (2006) J Phys Chem B 110:5515–5528
3. Spinelli A, Gonçalves RS (1990) Corr Sci 30:1235–1246
4. Olivera WX, Gonçalves RS (1992) J Braz Chem Soc 3:92–94
5. Vendrame ZB, Gonçalves RS (1998) J Braz Chem Soc 9:441–448
6. Mello LD, Gonçalves RS (2001) Corr Sci 43:457–470
7. Lucho AMS, Gonçalves RS, Azambuja DS (2002) Corr Sci 44:467–479
8. Martinez S, Stern I (2002) App Surf Sci 199:83–89
9. Manov S, Lamazouère AM, Áries L (2000) Corr Sci 42:1235–1248
10. Garrigues L, Pebere N, Dabosi F (1996) Electrochim Acta 41:1209–1215
11. El-Sherbini EEF, Wahaab SMA, Deyab M (2005) Mat Chem Phys 89:183–191
12. Talati JD, Desai MN, Shah NK (2005) Mat Chem Phys 93:54–64
13. Abdel-Gaber AM, Abdel-Rahman HH, Ahmed AM, Fathalla MH (2006) Anti-Corr Meth Mat 53:218–223
14. Chagas LV, Gonçalves RS (1996) Corrosion – NACE 52:653–658
15. El-Etre AY, Abdallah M, El-Tantawy ZE (2005) Corr Sci 47:385–395
16. Abioloa OK, Oforka NC, Ebenso EE, Nwinuka NM (2007) Anti-Corr Meth Mat 54:219–224
17. Machado TF, Antonow M, Gonçalves RS (2006) App Surf Sci 253:566–571
18. Blanc C, Freulon A, Lafont M-C, Kihn Y, Manowski G (2006) Corr Sci 48:3838–3851
19. Buccheidt RG, Martinez MA, Montes LP (2000) J Electrochem Soc 147:119–124
20. Bessone J, Salinas DR, Mayer C, Ebert M, Lorenz WJ (1992) Electrochim Acta 37:2283–2290
21. Frignani A, Zucchi F, Trabanelli G, Grassi V (2006) Corros Sci 48:2258–2273
22. Brett CMA (1990) J Appl Electrochem 20:1000–1003
23. Treacy GM, Rudd AL, Breslin CB (2000) J Appl Electrochem 30:675–683
24. Franceschetti DR, Macdonald JR (1977) J Electroanal Chem 82:271–301